



Death effector domain–containing protein (DEDD) is required for uterine decidualization during early pregnancy in mice

Mayumi Mori,¹ Miwako Kitazume,¹ Rui Ose,² Jun Kurokawa,¹ Kaori Koga,³ Yutaka Osuga,³ Satoko Arai,¹ and Toru Miyazaki¹

¹Laboratory of Molecular Biomedicine for Pathogenesis, Center for Disease Biology and Integrative Medicine, Faculty of Medicine, The University of Tokyo, Bunkyo-ku, Tokyo, Japan. ²Department of Human Genome Research, Kazusa DNA Research Institute, Kisarazu, Chiba, Japan. ³Department of Obstetrics and Gynecology, Faculty of Medicine, The University of Tokyo, Bunkyo-ku, Tokyo, Japan.

During intrauterine life, the mammalian embryo survives via its physical connection to the mother. The uterine decidua, which differentiates from stromal cells after implantation in a process known as decidualization, plays essential roles in supporting embryonic growth before establishment of the placenta. Here we show that female mice lacking death effector domain–containing protein (DEDD) are infertile owing to unsuccessful decidualization. In uteri of *Dedd*^{-/-} mice, development of the decidual zone and the surrounding edema after embryonic implantation was defective. This was subsequently accompanied by disintegration of implantation site structure, leading to embryonic death before placentation. Polyploidization, a hallmark of mature decidual cells, was attenuated in DEDD-deficient cells during decidualization. Such inefficient decidualization appeared to be caused by decreased Akt levels, since polyploidization was restored in DEDD-deficient decidual cells by overexpression of Akt. In addition, we showed that DEDD associates with and stabilizes cyclin D3, an important element in polyploidization, and that overexpression of cyclin D3 in DEDD-deficient cells improved polyploidization. These results indicate that DEDD is indispensable for the establishment of an adequate uterine environment to support early pregnancy in mice.

Introduction

Approximately 10%–15% of couples experience infertility during their reproductive years, owing mainly to implantation failure. Among the reasons underlying such failure, defective development of functional decidua at the implantation site within the uterus has recently been highlighted (1–3). In response to implantation, stromal cells immediately surrounding the mucosal crypt where the embryo is embedded proliferate extensively and undergo differentiation into polyploid decidual cells, forming an avascular primary decidual zone, followed by a broad, well-vascularized secondary decidual zone. It is believed that this decidual structure is important for the provision of nutrition to the developing embryo and also acts as a barrier against uncontrolled trophoblast proliferation until the placenta develops. Analyses of mutant mice that show female infertility, such as in knockout mice for homeobox A10 (*Hoxa10*) (4, 5) or IL-11 receptor (6), have contributed to the investigation of the molecular mechanisms involved in decidualization. Recent evidence has implicated cell-cycle regulation as being essential for both the proliferation and differentiation of stromal cells. In particular, Das and colleagues reported that cyclin D3–dependent activation of cyclin-dependent kinase 4 (Cdk4) or Cdk6 appears to be involved sequentially in those two events during decidua formation (7). In addition to these essential elements, in this report, we present data indicating that the death effector domain–containing (DED-containing) protein DEDD is indispensable for the maturation of decidual cells and support of female fertility in mice.

We previously found that the DEDD protein, initially described as a member of the DED-containing protein family, is associated with the Cdk1/cyclin B1 complex, thereby decreasing the kinase activity

of Cdk1 (8). This response impedes Cdk1-dependent mitotic progression, preserving synthesis of ribosomal RNA (rRNA) and protein and resulting in sufficient cell growth before cell division (8, 9). Consistently, depletion of DEDD results in a shortened mitotic duration, an overall decrease in the amount of cellular rRNA and protein, and decreased cell and body size (8, 9). In addition to the function of DEDD as a cell-cycle regulator, we recently determined that DEDD associates with S6K1 (10) and Akt (11), major elements of the signaling cascade involving mitogen-related PI3K. Such associations support the roles of S6K1 activity and Akt protein stability, respectively, in contributing to the maintenance of glucose homeostasis in the body (10, 11). Hence, DEDD is multifunctional and is involved in different physiological mechanisms. In fact, we found that female *Dedd*^{-/-} mice are infertile, and embryos of all DEDD genotypes die during early pregnancy within the *Dedd*^{-/-} uterus, whereas *S6K1*^{-/-} female mice, which also show a similar small phenotype and attenuated glucose homeostasis, show normal fertility (12). Given the phenotypic similarity of *Dedd*^{-/-} mice to other infertile mutant mice (4–6), this observation led us to address whether DEDD might also be involved in uterine decidualization.

In the present study, we assessed embryos implanted in *Dedd*^{-/-} uteri. In addition, we analyzed the maturation state of uterine decidual cells from *Dedd*^{-/-} mice in vitro and in vivo. We also studied the molecular mechanism underlying the inefficient decidualization of *Dedd*^{-/-} cells.

Results

Female *Dedd*^{-/-} mice are infertile. We found that *Dedd*^{-/-} female mice exhibited complete sterility when mated with males of any genotype (*Dedd*^{-/-}, *Dedd*^{+/-}, or *Dedd*^{+/+}), although *Dedd*^{-/-} offspring were born from the intercross of *Dedd*^{+/-} mice at a Mendelian ratio, and

Conflict of interest: The authors have declared that no conflict of interest exists.

Citation for this article: *J Clin Invest.* 2011;121(1):318–327. doi:10.1172/JCI44723.



Table 1
Female *Dedd*^{-/-} mice are infertile

Genotype		Offspring			Sum	n	Birth rate
Female	Male	+/+	+/-	-/-			
+/+	+/-	13 (46%)	15 (54%)	0 (0%)	28	6	4.67
+/+	-/-	0 (0%)	87 (100%)	0 (0%)	87	18	4.83
+/-	+/+	24 (51%)	23 (49%)	0 (0%)	47	10	4.70
+/-	+/-	108 (30%)	183 (51%)	66 (19%)	357	65	5.49
+/-	-/-	0 (0%)	47 (64%)	27 (36%)	74	17	4.35
-/-	+/+	0	0	0	0	23	0.00
-/-	+/-	0	0	0	0	37	0.00
-/-	-/-	0	0	0	0	12	0.00

The breeding efficiency in male-female combinations of various *DEDD* genotypes was investigated. Sum, total number of newborns; n, number of successful matings (with a vaginal plug); birth rate: sum/n.

Dedd^{-/-} male mice were fertile (Table 1). Mating efficiency was comparable in female *Dedd*^{-/-} mice and female mice of other genotypes, as assessed by vaginal plug formation (data not shown). The uterine *Dedd* mRNA level was upregulated after 4.5 dpc as assessed by quantitative RT-PCR (QPCR) (Figure 1A). An increase in *Dedd* expression was also observed in stromal cells differentiated to mature decidual cells in vitro in the presence of estrogen, progesterone (P4), and heparin-binding EGF-like growth factor (HB-EGF) (Figure 1B). Upregulation of *DEDD* expression along with the decidualization was also detected in human uterine stromal cells (Figure 1C). These results suggested that uterine *DEDD* is important after implantation and that the maturation of uterine decidual cells may be associated with *DEDD* expression.

Consistently, when 4.5-dpc uteri were analyzed with injection of blue dye (1% Chicago blue solution) (13), the number of implantation sites was comparable in *Dedd*^{-/-} and *Dedd*^{+/+} mice (6.8 ± 0.73 in *Dedd*^{-/-} mice and 7.4 ± 0.40 in *Dedd*^{+/+} mice; n = 5 each). In addition, the spacing and crowding of implanted embryos in the uterus was also similar in *Dedd*^{-/-} and *Dedd*^{+/+} mice (Figure 1D). Histologic analysis of 4.5-dpc *Dedd*^{-/-} uteri revealed normal embryonic implantation (Figure 1E). No difference was observed in the size of the edematous region and the decidual zone, which are formed in response to implantation (Figure 1E). Immunostaining for COX-2, an implantation site marker (14), corroborated the finding of normal embryonic implantation in *Dedd*^{-/-} and *Dedd*^{+/+} uteri (Figure 1E). Similarly, the mRNA level for *Ptgs2/Cox2* was comparable in *Dedd*^{-/-} and *Dedd*^{+/+} uteri, as assessed by QPCR with total RNA isolated from implantation sites (data not shown). However, anatomical analysis showed that in *Dedd*^{-/-} uteri, the number of living embryos decreased rapidly between 5.5 and 8.5 dpc (Figure 1F). At 9.5 dpc, the period of placenta formation, no living embryos were detected in *Dedd*^{-/-} uteri (Figure 1F). During this period, living embryos in *Dedd*^{-/-} uteri were of smaller size compared with those in *Dedd*^{+/+} uteri, and the difference in average embryo size between these two groups became more prominent at later dpc (Table 2). Thus, whereas implantation occurred normally in *Dedd*^{-/-} uteri, embryos showed growth defects and died by 9.5 dpc, before placenta formation. Note that serum levels of estrogen and P4, as well as mRNA levels for the receptor for each hormone (*Esr1* and *Pgr*, respectively) were similar in *Dedd*^{-/-} and *Dedd*^{+/+} females (Supplemental Figure 1; supplemental material available online with this article; doi:10.1172/JCI44723DS1). Preimplantation uterine histology was also comparable (Supplemental Figure 2). In addition, the proliferation of uter-

ine epithelial and stromal cells as well as expression induction of genes such as *Vegf* and *Lif* in response to estrogen were similar in *Dedd*^{-/-} and *Dedd*^{+/+} ovariectomized mice (Supplemental Figure 3). In addition, histologic ovarian morphology, ovulation, and intrauterine fertilization were normal in *Dedd*^{-/-} females (data not shown).

Defective decidualization and disintegrated structure of the implantation site in Dedd^{-/-} uteri. Histological analysis of 5.5-dpc uteri showed that the size of the decidual zone was smaller in *Dedd*^{-/-} compared with *Dedd*^{+/+} mice (Figure 2A). This was confirmed by immunostaining for the decidual marker tissue inhibitor of metal-

loproteinase 3 (TIMP3) (quantification also shown in Figure 2A) (15). Consistent with these results, mRNA levels for various genes that are highly expressed in decidual cells were decreased in *Dedd*^{-/-} compared with *Dedd*^{+/+} uteri, as assessed by QPCR with total RNA isolated from implantation sites (Figure 2B). Of these, the expression level of P4-sensitive bone morphogenetic protein 2 (*Bmp2*) gene was compromised at 5.5 d.p.c in *Dedd*^{-/-} uteri, whereas that of *Hoxa10*, upstream of *Bmp2* (5, 16, 17), was similar to that in *Dedd*^{+/+} uteri. In addition to the decidual zone, the size of the edematous region surrounding the decidual zone was also decreased in *Dedd*^{-/-} compared with *Dedd*^{+/+} mice (Figure 2A), suggesting that vascular permeability might be reduced in *Dedd*^{-/-} uteri.

Such attenuated development of the decidual zone in *Dedd*^{-/-} uteri was accompanied by disintegrated structure of the implantation site at later phases of pregnancy. At 7.5 dpc, a large proportion of decidual cells exhibited a shrunken shape, and marked bleeding was detected at the edge of the cavity in *Dedd*^{-/-} uteri (Figure 2C). In 8.5-dpc *Dedd*^{-/-} uteri, the structure of the outer wall of the embryonic cavity, which is supported by Reichert's membrane and trophoblastic giant cells (TGCs), had collapsed (Figure 2C), and irregular distribution of TGCs (i.e., invasion of TGCs into inner area of uteri) was more remarkable (Figure 2D). Such inadequate uterine environment may cause infertility in female *Dedd*^{-/-} mice.

Defective polyploidy in Dedd^{-/-} decidual cells. We next assessed the state of polyploidy, a hallmark of mature decidual cells, in *Dedd*^{-/-} and *Dedd*^{+/+} uterine stromal cells undergoing decidualization in vitro in the presence of estrogen, P4, and HB-EGF. As shown in Figure 3A, at days 3 and 7, the proportion of multinuclear cells observed microscopically was more than 50% smaller in *Dedd*^{-/-} cells than in *Dedd*^{+/+} cells. Consistent with this result, analysis of these cells by the flow cytometer after DNA staining revealed a significant decrease in the proportion of cells that possessed more than 4 copies of genomic DNA (indicated as 4n and 8n) in *Dedd*^{-/-} compared with *Dedd*^{+/+} cells (Figure 3B). Similar results were obtained in vivo in cells isolated from 4.5-dpc implantation sites in *Dedd*^{-/-} and *Dedd*^{+/+} uteri by collagenase treatment (Figure 3C). Thus, the defect in decidualization observed in *Dedd*^{-/-} uteri was associated with attenuated terminal maturation with less polyploidy.

In contrast, the proliferative status of uterine stromal cells in response to implantation was not different in *Dedd*^{-/-} and *Dedd*^{+/+} mice, as judged by the comparable cell number isolated from implantation sites at 4.5 dpc (1.08 × 10⁶ ± 0.15 × 10⁶ in *Dedd*^{-/-}

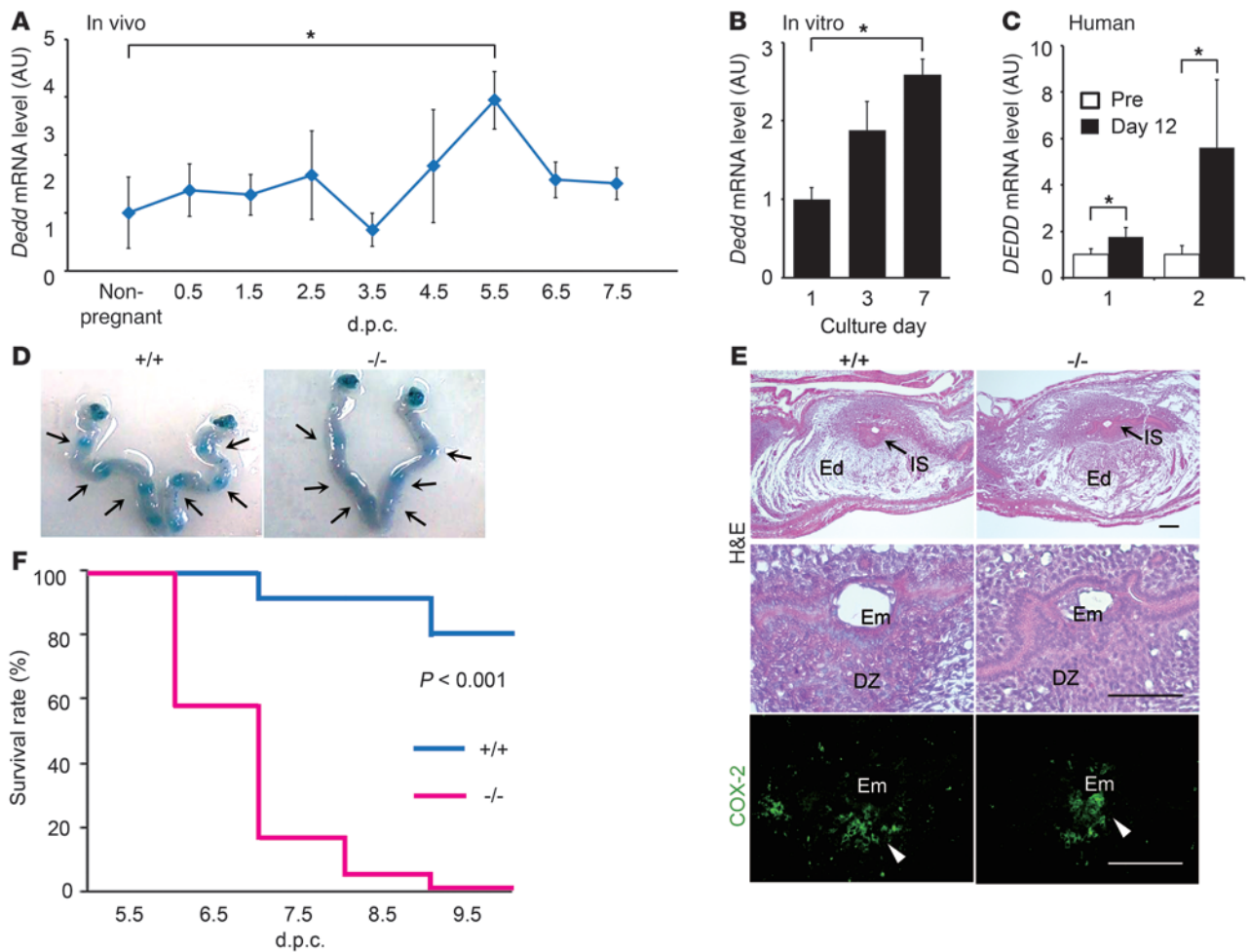


Figure 1 Postimplantation embryonic death in *Dedd*^{-/-} uteri. (A–C) Increase in *Dedd* mRNA level in response to implantation in wild-type mouse (A) or in vitro decidualization in mouse uterine stromal (B) and human endometrial (C) cells, assessed by QPCR. Values were normalized to those of β -actin or GAPDH and are presented as relative expression to those of nonpregnant (A), day 1 (B), or undifferentiated (C) controls. Pre, undifferentiated cells; Day 12, decidualized cells at 12 days after the differentiation induction. In C, results from triplicate experiments using specimens from two individuals (1 and 2) are shown. Error bars indicate SEM. (D) Embryo spacing and crowding were assessed by blue dye injection. Representative photos of the uteri are shown. (E) Histologic analysis of implantation sites at 4.5 dpc in *Dedd*^{+/+} (+/+) and *Dedd*^{-/-} (-/-) uteri. Sections were stained with H&E or immunostained for COX-2. Em, embryo; DZ, decidual zone; Ed, edematous region (outside of DZ, white zone). Positive signals for COX-2 are indicated by arrowheads. Scale bars: 200 μ m. (F) Survival rates of embryos during early gestation (Kaplan-Meier method). When embryo bodies were observed, regardless of size, they were regarded as “alive,” whereas degenerated masses or those with scars at implantation sites were regarded as “dead.” $n = 75$ for *Dedd*^{+/+} and $n = 44$ for *Dedd*^{-/-} uteri; log-rank, $\chi^2 = 13.2$. * $P < 0.05$.

mice and $1.21 \times 10^6 \pm 0.075 \times 10^6$ in *Dedd*^{+/+} mice; $n = 3$ each). Consistent with this result, when decidualizing stromal cells were challenged in vitro with 5-ethynyl-2'-deoxyuridine (EdU; a nucleotide analog of thymidine), the proportion of EdU-incorporated cells was equivalent in *Dedd*^{-/-} and *Dedd*^{+/+} cells (Supplemental Figure 4A). Also, in vivo, 5.5-dpc implantation sites in *Dedd*^{-/-} and *Dedd*^{+/+} uteri stained similarly for Ki67, which identifies proliferating cells (Supplemental Figure 4B).

Decreased Akt level in Dedd-/- uteri and increase in polyploidy by Akt expression in Dedd-/- decidual cells. As we reported previously, the amount of Akt (all isoforms) is decreased in various *Dedd*^{-/-} tissues, owing to decreased Akt protein stability (11). Notably, implantation sites in 5.5-dpc *Dedd*^{-/-} uteri also showed decreased levels of Akt protein compared with those in *Dedd*^{+/+} uteri, as assessed

by immunoblotting with a pan-Akt antibody (Figure 4A). Parallel results were also obtained using in vitro decidualizing cells (Supplemental Figure 5). Signal for activated Akt phosphorylated at Thr308 was also decreased (Figure 4A, p-Akt). As we observed in mouse embryonic fibroblasts (MEFs) and other tissues (11), mRNA levels for *Akt1* and *Akt2* did not decrease in these cells (data not shown). To test whether the decrease in Akt protein was essential for the defect in polyploidy observed in *Dedd*^{-/-} decidual cells (Figure 3), Akt-1 was overexpressed in in vitro differentiating *Dedd*^{-/-} uterine stromal cells, and polyploidy was analyzed. As expected, the proportion of polynuclear cells was significantly increased by forced Akt-1 expression (Figure 4B). Thus, a decrease in Akt protein level appeared to be responsible for the inefficient decidualization observed in *Dedd*^{-/-} uteri.



Table 2
Embryo size within *Dedd*^{+/+} and *Dedd*^{-/-} uteri

	Maternal genotype	Embryo size (mm ³)	n
Day 5.5	+/+	0.0059 ± 0.0014	9
	-/-	0.0039 ± 0.0012 ^A	9
Day 6.5	+/+	0.17 ± 0.014	5
	-/-	0.044 ± 0.0096 ^B	12
Day 7.5	+/+	0.51 ± 0.070	19
	-/-	0.25 ± 0.099 ^A	11
Day 8.5	+/+	>5.00	11
	-/-	1.00 ± 0.33	7

Both *Dedd*^{+/+} (+/+) females and *Dedd*^{-/-} (-/-) females were mated with *Dedd*^{+/+} males. Therefore, embryos in *Dedd*^{+/+} uteri were either *Dedd*^{+/+} or *Dedd*^{+/+}, whereas those in *Dedd*^{-/-} uteri were all *Dedd*^{-/-}. There was no significant difference in the size among the *Dedd*^{-/-} and *Dedd*^{+/+} embryos in *Dedd*^{+/+} uteri. ^AP < 0.05, ^BP < 0.001.

Dedd associates with cyclin D3 and supports its protein stability. Of the multiple functions of Akt, control of the cell cycle via regulation of D-type cyclins in terms of gene expression, protein stability, and localization within the cell has been documented in different physiologic and pathologic situations (18). Das and colleagues recently implicated cyclin D3 as a key regulator of polynuclearization (7, 19, 20). In addition, Garcia-Morales et al. showed that the protein stability of cyclin D3 is downregulated by rapamycin, an inhibitor of mammalian target of rapamycin (mTOR), downstream of Akt in the PI3K signaling pathway (21). This suggests that the decrease in Akt protein in the absence of DEDD might influence cyclin D3, resulting in a defect in polyploidy. To test this, we stained *Dedd*^{-/-} and *Dedd*^{+/+} uteri for cyclin D3 at 5.5 dpc. As shown in Figure 5A, *Dedd*^{-/-} decidua harbored fewer cyclin D3-positive cells. This decrease in cyclin D3 was confirmed by immunoblotting (Figure 5B). However, the mRNA level for cyclin D3 was similar in *Dedd*^{-/-} and *Dedd*^{+/+} uteri at 5.5 d.p.c (Figure 5C), suggesting that the stability of cyclin D3 is affected in *Dedd*^{-/-} cells. Therefore, we measured the half-life of cyclin D3 protein in in vitro differentiating stromal cells at day 3. Importantly, the amount of cyclin D3 protein started to decrease within 30 minutes in *Dedd*^{-/-} cells but not in *Dedd*^{+/+} cells (Figure 5D). By 90 minutes, the protein level of cyclin D3 was more than 3-fold lower in *Dedd*^{-/-} compared with *Dedd*^{+/+} cells (Figure 5D). The presence of MG132, a proteasome inhibitor, tempered the decrease observed in *Dedd*^{-/-} cells (Figure 5D). Thus, lack of DEDD resulted in instability of cyclin D3. As in the case of Akt, increase in cyclin D3 protein by overexpression improved polyploidy in *Dedd*^{-/-} decidual cells (Figure 5E), indicating that a decrease in cyclin D3 protein level also appeared to be involved in the inefficient decidualization observed in *Dedd*^{-/-} uteri.

Such a relationship among DEDD, cyclin D3, and Akt was also supported by an in situ mRNA analysis using 5.5- and 7.5-dpc *Dedd*^{+/+} uteri, which demonstrated coexpression of these 3 genes at the decidual zone cells in vivo (Figure 6A). Furthermore, DEDD associated with cyclin D3. This is similar to our previous observations that DEDD binds to various proteins such as cyclin B1, S6K1, and Akt (8–11). As shown in Figure 6B, immunoprecipitation in HEK293T cells expressing both FLAG-tagged cyclin D3 and hemagglutinin-tagged (HA-tagged) DEDD showed that the two proteins coprecipitated, indicating that DEDD may facilitate a complex with cyclin D3. Therefore, DEDD might support the stability of cyclin D3 by two independent pathways: maintenance

of the Akt protein level and direct formation of a DEDD/cyclin D3 complex. HA-tagged DEDD also coprecipitated with FLAG-tagged Cdk4 and Cdk6 (Figure 6B). Endogenous DEDD was also coprecipitated with cyclin D3, Cdk4, or Cdk6, when tested using protein isolated from implantation sites of 5.5-dpc uteri (Figure 6C). Similar to our observation that DEDD associates with Cdk1/cyclin B1 via direct binding to cyclin B1, DEDD might form a complex with Cdk4/cyclin D3 and Cdk6/cyclin D3, both of which are essential for the regulation of decidualization (9), via a direct association with cyclin D3.

Discussion

A new role for DEDD in uterine decidualization and female fertility. Results of the present study implicate DEDD as an indispensable element in supporting early pregnancy. First, DEDD was expressed in decidual cells, and its absence decreased the Akt protein level in these cells. Second, the lack of DEDD decreased the stability of cyclin D3. Third, *Dedd*^{-/-} stromal cells showed defective polyploidy during decidualization. Fourth, in *Dedd*^{-/-} uteri, inefficient polyploidy disturbed development of the decidual zone, which was accompanied by disintegrated structure of the implantation site. As a result of these defects, *Dedd*^{-/-} uteri cannot support embryonic growth before the development of the placenta, resulting in complete infertility of *Dedd*^{-/-} female mice.

The decidual cell polyploidy, which is a hallmark of mature decidual cells particularly in mice, is characterized by the formation of large mono- or binucleated cells, consisting of DNA with multiples of the haploid complement (22–24). Although it has been suggested that various biological processes including metabolic activity are associated with the polyploidy (25), the physiological significance of this event in uterine decidualization remains poorly understood. Complete infertility in female *Dedd*^{-/-} mice whose decidua showed a normal proliferative activity but less polyploidy may suggest the functional importance of polyploidy for the support of embryonic growth during early pregnancy.

It could be argued that the general effect of DEDD deficiency, such as decreased body size and mild attenuation of insulin production (8–11), might cause infertility. However, this is unlikely, given that female *S6K1*^{-/-} mice, which show a similar (or even more advanced) phenotype regarding body size and insulin production, remain fertile (12). Similarly, although *Akt1*^{-/-} mice also showed fetal growth impairment due to placental inefficiency, adult females are fertile (26).

Association of DEDD with decidual polyploidy via support of Akt and cyclin D3 stability. One reason why the absence of DEDD causes infertility appears to be the decrease in the amount of Akt protein in uterine stromal/decidual cells. Recent evidence in humans and mice suggests that Akt may play a role in the regulation of decidualization and in the survival of decidual cells. Of note, Hirota et al. showed increased decidual polyploidy with upregulation of Akt phosphorylation in mice with deficiency for p53 restricted to the uterus (27). As we reported previously, DEDD forms a complex with Akt and heat shock protein 90 (Hsp90) and stabilizes all isoforms of Akt protein (11). It is possible that defective protein stability of cyclin D3 may be brought about, in part, by a decrease in Akt, based on the facts that D-type cyclins are substrates for Akt, cyclin D3 is regarded as a major regulator of polyploidy, and the deficient polyploidy observed in *Dedd*^{-/-} cells was improved by forced expression of Akt-1. Nevertheless, the precise machinery whereby Akt influences the stability of cyclin D3 is not yet clear.

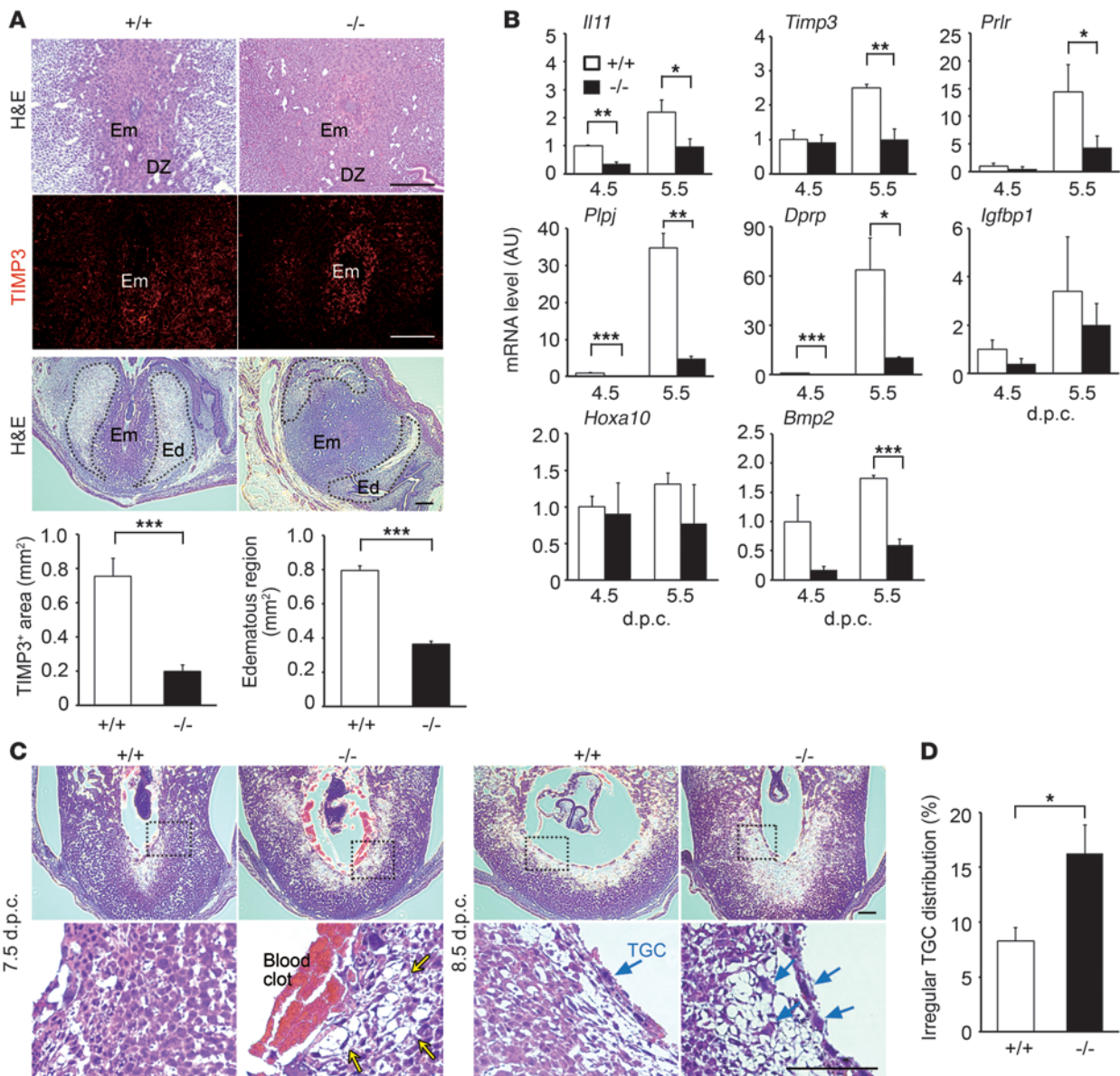


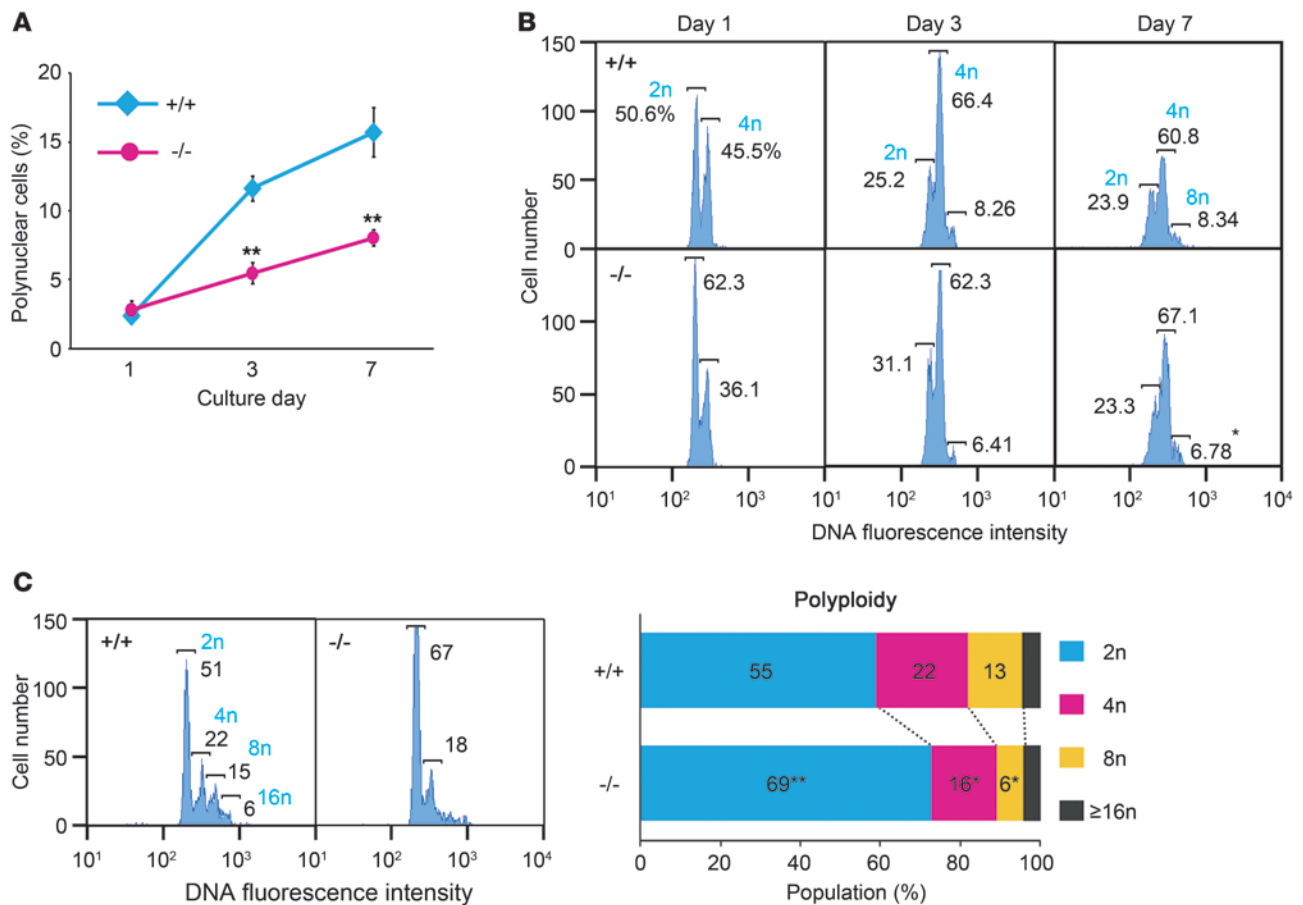
Figure 2

Defective decidualization in *Dedd*^{-/-} uteri. (A) Implantation sites of 5.5-dpc *Dedd*^{+/+} and *Dedd*^{-/-} uteri were stained with H&E or immunostained for TIMP3. Scale bars: 200 μ m. Quantification of decidual zone (TIMP3-positive area) and edematous region is also presented. At least 10 different sections in 3 different implantation sites were analyzed for each. Error bars indicate SEM. (B) mRNA levels of various genes that are highly expressed in decidua were analyzed by QPCR with total RNA isolated from 3 different implantation sites at 4.5 or 5.5 dpc. Values were normalized to those of β -actin and are presented as relative expression to 4.5-dpc *Dedd*^{+/+} mice. Error bars indicate SEM. *Prlr*, prolactin receptor; *Plpj*, prolactin-like protein J; *Dprp*, decidual prolactin-related protein; *Igfbp1*, IGF-binding protein 1. (C) Histologic analysis of 7.5- and 8.5-dpc uteri (H&E staining). Higher magnification of the boxed area in the respective upper panel is presented in the lower panel. Arrows at 7.5 dpc indicate shrunken cells in *Dedd*^{-/-} uterus. TGCs are denoted by blue arrows. Scale bars: 200 μ m. (D) Irregular distribution of TGCs in *Dedd*^{-/-} uterus. TGC numbers at the antimesometrial region of implantation sites were determined microscopically. At least 10 sections from 3 different specimens were examined. Data are shown as relative proportion of TGCs showing irregular distribution (invasion into the inner area). Error bars indicate SEM. * $P < 0.05$, ** $P < 0.01$, *** $P < 0.001$.

Further studies are required to address the molecular mechanism. Interestingly, DEDD associates with cyclin D3; this might contribute structurally to the protein stability of cyclin D3.

Because cyclin D3-deficient mice do not show complete infertility, as observed in *Dedd*^{-/-} mice (19, 28), a combination of various defects at the implantation site in addition to inefficient

polyploidy — such as inadequate development of the edematous region (Figure 2A) and disintegrated structure of the implantation site at 7–8 d.p.c (Figure 2C) — might contribute to the overall infertility observed in *Dedd*^{-/-} mice. These defects may also result from the decreased Akt level, given that Akt has diverse functions, including the maintenance of vascular permeability and an

**Figure 3**

Attenuated polyploidy in *Dedd*^{-/-} decidual cells. **(A)** In vitro decidualizing uterine stromal cells were stained with Hoechst to identify nuclei after different times in culture, and the number of polynuclear cells among 600 cells was counted microscopically. Analysis was performed by 3 independent researchers. **(B and C)** Quantification of DNA in in vitro decidualizing uterine stromal cells **(B)** or ex vivo stromal cells isolated from 4.5-dpc implantation sites **(C)**. Cells were stained with Hoechst and analyzed by flow cytometry. Three independent experiments were performed, and a representative set of profiles is presented. In **C**, the average sizes for 2n, 4n, 8n, and ≥16n populations are also presented (right panel). ***P* < 0.01.

antiapoptotic effect, in addition to regulation of the cell cycle (29–31). It is also noteworthy that no reproductive defects have been reported in mice deficient in Akt-1, -2, or -3, with the exception of two reports that *Akt1*^{-/-} mice harbor a partial defect in follicular development within the ovary (32, 33). Thus, each Akt isoform may be functionally redundant in supporting fertility, given that *Dedd*^{-/-} mice in which levels of all isoforms of Akt are decreased show a dramatic uterine defect (11). Our finding that the back-expression of Akt-1 efficiently recovered polyploidy in *Dedd*^{-/-} stromal cells may support this idea. Unfortunately, mice doubly or triply deficient for multiple types of Akt die before they reach reproductive age (34). Future creation and analysis of conditional knockout mice in which various types of Akt are specifically deficient in the uterus will help to elucidate the involvement of Akt in fertility.

Perspectives. Our present findings identifying DEDD as an indispensable element in support of early pregnancy might shed light on the pathogenesis of infertility of unknown cause. Indeed, *DEDD* expression in uterine stromal cells increases along with decidualization both in mice and humans. In women experiencing implantation failure, one-third of the failures have been attributed to the embryo itself (35). Although the remaining two-

thirds of failures appear to be the result of an inadequate uterine environment, the precise defect is often unknown. Thus, it may be worth addressing whether DEDD dysfunction is present in infertile women, either genetically or functionally, in uterine stromal cells. This may contribute to the development of new therapeutic strategies for infertility, though association of DEDD function with polyploidization as well as Akt and cyclin D3 in humans certainly needs to be further assessed.

Methods

Mice and human specimens. *Dedd*^{-/-} mice had been cross-bred to C57BL/6 for 17 generations before being used for experiments. Female mice of 2–6 months of age were used. The day of the vaginal plug was considered as 0.5 dpc. Pseudopregnant mice were produced by mating female mice with vasectomized male mice of the CD-1 strain. All mice were maintained under specific pathogen-free conditions. All animals used in the experiments were cared for in accordance with institutional guidelines. Human endometrial tissue was obtained from women with benign diseases. The experimental procedures were approved by the institutional review board of the University of Tokyo, and all women provided written informed consent for the use of their endometrial tissue.

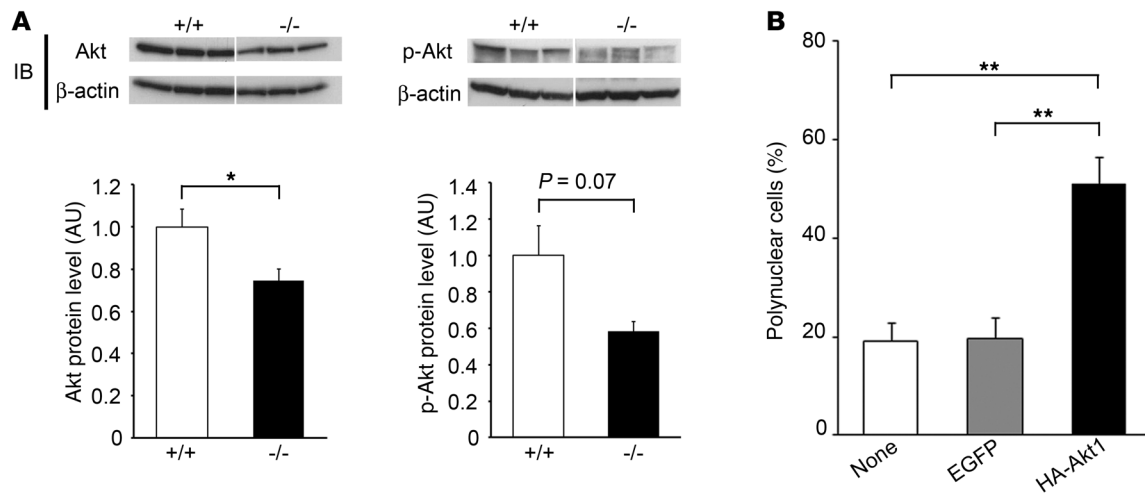


Figure 4

Involvement of Akt level in defective polyploidy in *Dedd*^{-/-} decidual cells. (A) Immunoblotting of *Dedd*^{+/+} and *Dedd*^{-/-} uteri at 5.5 dpc for total Akt (left) and phosphorylated Akt (at Thr308, right). Three mice were analyzed. Quantification was performed with NIH Image J software. Values are presented as protein levels relative to those from *Dedd*^{+/+} uteri. Error bars indicate SEM. (B) In vitro decidualizing *Dedd*^{-/-} stromal cells were transfected with expression vector for HA-Akt1 or control EGFP at day 2. At day 5, cells were stained for HA and Hoechst; thereafter, the proportion of polynuclear cells among more than 100 HA-positive cells was evaluated microscopically. Average results from 4 independent sets of experiment are presented. Error bars indicate SEM. **P* < 0.05, ***P* < 0.01.

Reagents and antibodies. Antibodies and reagents used were as follows. Primary antibodies were: anti-COX-2 (polyclonal, Cell Signaling Technology); anti-TIMP3 (W-18, Santa Cruz Biotechnology Inc.); anti-Akt (pan) (11E7, Cell Signaling Technology); anti-Ki67 (SP6, Thermo Scientific); anti-phospho-Akt (Thr308) (244F9, Cell Signaling Technology); anti-cyclin D3 (C-16, Santa Cruz Biotechnology Inc.) for immunohistochemistry; anti-cyclin D3 (DCS-22, Thermo Scientific) for immunoblotting and immunoprecipitation; anti-Cdk4 (DCS-35, Thermo Scientific); anti-Cdk6 (DCS-83, Thermo scientific); anti-β-actin (ACTN05 [C4], Abcam); anti-HA high-affinity antibody (3F10, Roche); and anti-FLAG antibody (M2, Sigma-Aldrich). Secondary antibodies and related reagents were: Alexa Fluor 488-conjugated anti-rabbit IgG antibody (Invitrogen); Alexa Fluor 546-conjugated anti-goat IgG antibody (Invitrogen); Hoechst 33258 and Hoechst 33324 (Invitrogen); Protein Block Serum-Free (Dako Cytomation); normal goat serum (Wako); Mayer’s hematoxylin (Muto Pure Chemicals Co. Ltd.); eosin Y solution (Sigma-Aldrich); HRP-conjugated anti-mouse IgG (Pierce); and HRP-conjugated anti-rabbit IgG (Pierce).

Analysis of ovulation and fertilization. Briefly, superovulation was induced by intraperitoneal injection of pregnant mare serum gonadotropin (PMSG) (at -2.5 dpc; 5 IU/mouse) and human chorionic gonadotropin (hCG) (at -0.5 dpc; 5 IU/mouse). Oviducts from mated females were flushed with M2 medium at 0.5 dpc. Under a microscope, numbers of eggs were determined, and fertilization efficiency was evaluated by morphology of the eggs (i.e., having 2 nuclei or a fused large nucleus).

Histologic and immunohistochemical analysis. Uterine specimens were fixed by infusion of 4% PFA. For immunohistochemistry, deparaffinized sections were boiled in 10 mM sodium citrate buffer, pH 6.0, by microwave for 10 minutes. After blocking, sections were incubated with primary antibodies at 4°C for 16 hours, followed by secondary antibodies at room temperature for 1 hour. Samples were counterstained with Hoechst 33258. The areas of TIMP3-positive region and edematous region were measured by ImageJ software (NIH). Similarly, the embryonic area was measured. The size of each embryo was calculated as the sum of the embryonic area multiplied by its thickness (10 μm/section).

In situ hybridization. A 433-bp DNA fragment corresponding to the nucleotide positions 81–513 of mouse *Dedd* was subcloned into pGEMT-Easy vector (Promega) and was used for generation of sense or antisense RNA probes. A 431-bp DNA fragment corresponding to the nucleotide positions 1082–1512 of mouse *cyclin D3* and a 694-bp DNA fragment corresponding to the nucleotide positions 1851–2544 of mouse *Akt1* were similarly prepared. Paraffin-embedded uterine sections (6 μm) were hybridized with digoxigenin-labeled RNA probes at 60°C for 16 hours. The bound label was detected using NBT-BCIP, an alkaline phosphate color substrate. The sections were counterstained with Kernechtrot (Muto Pure Chemicals Co. Ltd.).

Primary culture of uterine stromal cells. The isolation and culture of mouse uterine stromal cells were performed as previously described (36). Briefly, uterine horns on day 3.5 of pseudopregnancy were cut and washed in HBSS (Invitrogen) without Ca²⁺/Mg²⁺ and phenol red but containing 100 U/ml penicillin and 100 μg/ml streptomycin (Pen Strep; Invitrogen) and 2.5 μg/ml amphotericin B (Sigma-Aldrich). Tissues were digested in HBSS containing 6 mg/ml dispase (Invitrogen) and 25 mg/ml pancreatin (Sigma-Aldrich) and subsequently treated with 0.5 mg/ml collagenase (Sigma-Aldrich). The digested cells were passed through a 70-μm nylon filter to eliminate clumps of epithelial cells and were plated at 5 × 10⁵ cells per 25 cm². For in vitro decidualization, the adherent cells were cultured in phenol red-free DMEM and Ham’s F-12 nutrient mixture (DMEM/F-12, 1:1) (Invitrogen) with 1% charcoal-stripped FBS (Invitrogen) and antibiotics, 17β-estradiol (E2, 10 nM) (Sigma-Aldrich), P4 (1 μM) (Sigma-Aldrich), and HB-EGF (30 ng/ml) (Sigma-Aldrich). The induction of differentiation was continued for 7 days without changing medium. Isolation and differentiation of human endometrial stromal cells were performed as described previously (37). Cells were treated with phenol red-free DMEM/F-12 containing 5% charcoal-stripped FBS, antibiotics, E2 (10 ng/ml), and P4 (100 ng/ml) for 12 days. Media were replenished every 3 days.

Analysis of cell cycle and polyploidization. Cell cycle was analyzed using the Click-iT EdU kit (Invitrogen). Cultured uterine stromal cells were harvested at days 1, 3, and 7 after 10 μM EdU incorporation for 2 hours each. Trypsinized cells were fixed with 4% PFA and permeabilized with saponin. Incorporated EdU

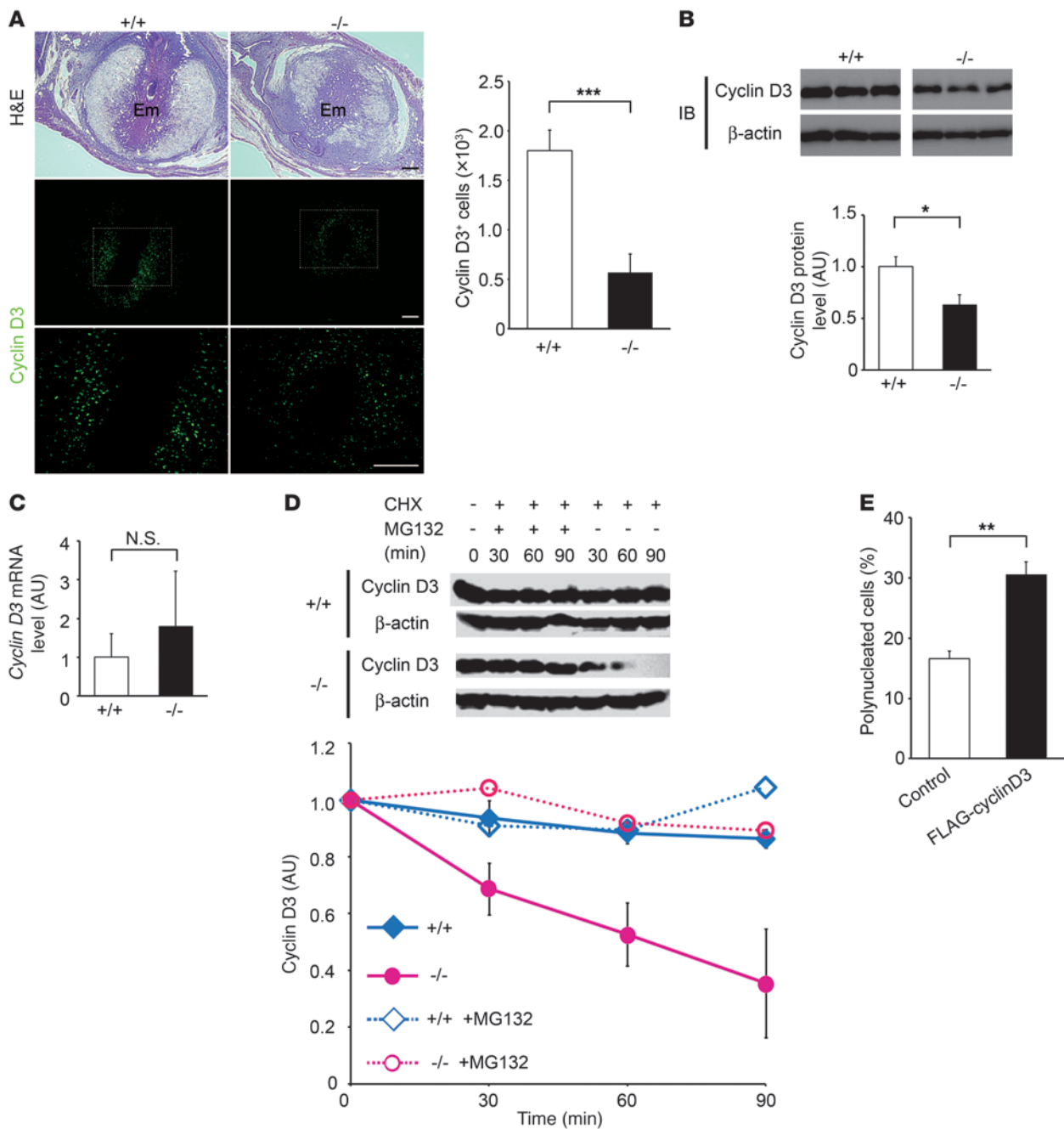


Figure 5

Decreased stability of cyclin D3 protein in *Dedd*^{-/-} decidual cells. (A) At 5.5 dpc, implantation sites in *Dedd*^{+/+} and *Dedd*^{-/-} uteri were immunostained for cyclin D3. Bottom panels show higher magnifications of the dotted area in the middle panels. Scale bars: 200 μm. Graph on the right: Cyclin D3-positive cells within an implantation site were counted and compared in at least 4 different sections, and the means are presented. Error bars indicate SEM. (B) Immunoblotting of *Dedd*^{+/+} and *Dedd*^{-/-} uteri at 5.5 dpc for cyclin D3 and quantification of results. Three mice were analyzed. Error bars indicate SEM. (C) mRNA level for *cyclin D3* in 5.5-dpc implantation sites. No significant decrease in mRNA level was detected in *Dedd*^{-/-} cells and tissues (*n* = 3 for each). (D) Protein degradation assay for cyclin D3. Uterine stromal cells at day 3 of in vitro decidualization were treated with cycloheximide (CHX; 50 μM) for the indicated periods in the presence or absence of proteasome inhibitor MG132 (10 μM). At each time point, cells were harvested, and the lysate was analyzed for cyclin D3 by immunoblotting. The amount of cyclin D3 protein at each time point was normalized to that of β-actin and is presented as relative level to that at pretreatment (0 minutes) in *Dedd*^{+/+} or *Dedd*^{-/-} cells. Three independent experiments were performed, and representative blots are presented. Error bars indicate SEM. (E) In vitro decidualizing *Dedd*^{-/-} stromal cells were transfected with expression vector for FLAG-cyclin D3 at day 2. At day 5, cells were stained for FLAG and Hoechst; thereafter, the proportion of polynuclear cells among more than 100 FLAG-positive cells was evaluated microscopically. Average results from 4 independent sets of experiment are presented. Error bar indicate SEM. **P* < 0.05, ***P* < 0.01, ****P* < 0.001.

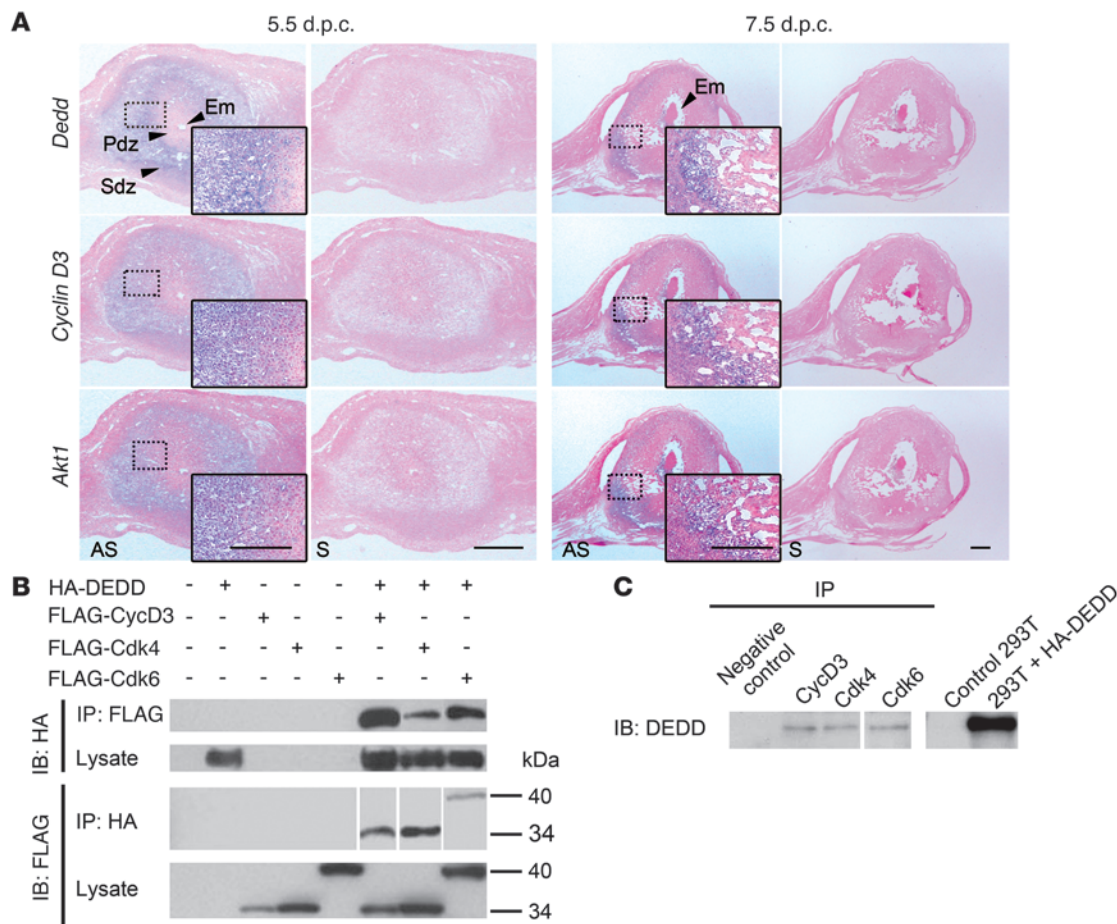


Figure 6

The association of DEDD with cyclin D3. **(A)** In situ mRNA analysis for *Dedd*, *cyclin D3*, and *Akt1* in 5.5- and 7.5- dpc wild-type mouse uteri. Microphotographs at a higher magnification are also presented. AS, antisense probe; S, sense control probe; PdZ, primary decidual zone; Sdz, secondary decidual zone. Scale bars: 500 μ m. **(B)** Binding study. HA-tagged DEDD and FLAG-tagged cyclin D3, Cdk4, or Cdk6 were expressed in HEK293T cells, and association of HA-DEDD and each FLAG-tagged protein was evaluated by a coimmunoprecipitation assay with anti-HA or anti-FLAG antibody. **(C)** Coprecipitation of endogenous DEDD with cyclin D3, Cdk4, or Cdk6 from lysates of 5.5-dpc uterine implantation sites. Precipitates were immunoblotted with an anti-DEDD antibody. HEK293T cells with or without transfection of HA-tagged DEDD were used as controls.

was detected by an alkylation reagent conjugated with Alexa Fluor 488. DNA content was quantitatively detected by subsequent staining with Hoechst 33342. At least 10,000 cells for each sample were analyzed by flow cytometry. For evaluation of polyploidy, cells were cultured in a 4-well chamber and stained with Hoechst after fixation with 4% PFA. Multinucleated cells were calculated under a fluorescence microscope and counted by 3 independent researchers in a blinded fashion from more than 600 total cells each.

Flow cytometry (analysis of cell DNA contents). In vitro decidualizing cells were stained with Hoechst 33342 and analyzed for DNA content by an LSR II flow cytometer (BD). At least 10,000 cells were analyzed for each. For ex vivo cells, 4.5-dpc uterine implantation sites were digested by a collagenase treatment, and purified single cells were stained with Hoechst 33342. The large stromal cell population was gated, and at least 1,000 cells were analyzed for DNA content.

Akt and cyclin D3 overexpression in decidual cells. Uterine stromal cells at day 2 of culture in the presence of E2, P4, and HB-EGF were transfected with a pCruz-HA-Akt1, pFLAG-cyclinD3, or a mock expression vector by using Lipofectamine 2000 (Invitrogen). At day 5, cells were fixed with 4% PFA and permeabilized with 0.25% Triton X-100. The transfected cells

were detected by anti-HA high-affinity antibody or anti-FLAG antibody conjugated with Cy3. Multinucleated cells were counted under a fluorescence microscope after Hoechst staining.

Protein degradation assay. Day 3 in vitro decidualizing stromal cells were treated with 50 μ M cycloheximide (Sigma-Aldrich) in the presence or absence of 10 μ M MG132 (Sigma-Aldrich) and were harvested at the indicated time points. Cells were lysed in a lysis buffer (1% NP-40, 150 mM NaCl, 50 mM Tris-HCl pH 7.4, 1 mM sodium orthovanadate, 1 mM sodium fluoride, and Complete Mini [Roche]) and used for immunoblotting.

Coimmunoprecipitation assay. HEK293T cells were transfected with pCAG-DEDD-HA, pFLAG-cyclin D3, pFLAG-Cdk4, or pFLAG-Cdk6 by electroporation. Cells were lysed and incubated with anti-HA or anti-FLAG beads for 16 hours at 4°C. Precipitates were analyzed for the presence of coprecipitated molecule by immunoblotting using anti-FLAG or anti-HA antibody. For the binding of endogenous DEDD with cyclin D3, Cdk4, or Cdk6, 5.5-dpc uterine implantation sites were homogenized in lysis buffer and incubated with anti-cyclin D3, anti-Cdk4, or anti-Cdk6 antibody bound to protein G beads. Precipitates were immunoblotted with an anti-DEDD polyclonal antibody prepared in-house (8).



Quantitative and semiquantitative RT-PCR. QPCR was performed using Power SYBR Green PCR Master Mix (Applied Biosystems) and the ABI Prism 7000 Sequence Detection System (Applied Biosystems). Results were analyzed by the $\Delta\Delta C_t$ method, in which the C_t s of β -actin were used for normalization. Primer sequences are detailed in Supplemental Table 1. For semiquantitative PCR shown in Supplemental Figure 3, primers are shown in Supplemental Table 2.

Statistics. All statistical analyses were performed using 2-tailed Student's *t* test. Standard deviation and variance of every data set were calculated, and the homoscedasticity was confirmed by *F* test. *P* values less than 0.05 were considered significant.

Acknowledgments

We thank to A. Kodama, T. Fujii, Y. Taketani, H. Kurihara, and Y. Kurihara (Tokyo), M. Noguchi (Sapporo), and A. Nishijima, for technical assistance and constructive discussion; Genostaff Co.

Ltd. for in situ mRNA hybridization; and M. Miyamoto for administrative assistance. This work was supported by the Global COE Research Program, Uehara Memorial Foundation (to T. Miyazaki), and the Kanzawa Research Medical Foundation (to S. Arai).

Received for publication August 12, 2010, and accepted in revised form October 20, 2010.

Address correspondence to: Toru Miyazaki, Laboratory of Molecular Biomedicine for Pathogenesis, Center for Disease Biology and Integrative Medicine, Faculty of Medicine, The University of Tokyo, 7-3-1 Hongo, Bunkyo-ku, Tokyo 113-0033, Japan. Phone: 81.3.5841.1435; Fax: 81.3.5841.1438; E-mail: tm@m.u-tokyo.ac.jp.

Miwako Kitazume's present address is: Division of Developmental Genetics, National Institute of Genetics, Mishima, Shizuoka, Japan.

1. Wang H, Dey SK. Roadmap to embryo implantation: clues from mouse models. *Nat Rev Genet.* 2006;7(3):185–199.
2. Dey SK, et al. Molecular cues to implantation. *Endocr Rev.* 2004;25(3):341–373.
3. Das SK. Cell cycle regulatory control for uterine stromal cell decidualization in implantation. *Reproduction.* 2009;137(6):889–899.
4. Satokata I, Benson G, Maas R. Sexually dimorphic sterility phenotypes in Hoxa10-deficient mice. *Nature.* 1995;374(6521):460–463.
5. Lim H, Ma L, Ma WG, Maas RL, Dey SK. Hoxa-10 regulates uterine stromal cell responsiveness to progesterone during implantation and decidualization in the mouse. *Mol Endocrinol.* 1999;13(6):1005–1017.
6. Robb L, Li R, Hartley L, Nandurkar HH, Koentgen F, Begley CG. Infertility in female mice lacking the receptor for interleukin 11 is due to a defective uterine response to implantation. *Nat Med.* 1998;4(3):303–308.
7. Tan J, Raja S, Davis MK, Tawfik O, Dey SK, Das SK. Evidence for coordinated interaction of cyclin D3 with p21 and cdk6 in directing the development of uterine stromal cell decidualization and polyploidy during implantation. *Mech Dev.* 2002;111(1–2):99–113.
8. Arai S, et al. Death-effector domain-containing protein DEDD is an inhibitor of mitotic Cdk1/cyclin B1. *Proc Natl Acad Sci U S A.* 2007;104(7):2289–2294.
9. Miyazaki T, Arai S. Two distinct controls of mitotic cdk1/cyclin B1 activity requisite for cell growth prior to cell division. *Cell Cycle.* 2007;6(12):1419–1425.
10. Kurabe N, et al. The death effector domain-containing DEDD supports S6K1 activity via preventing Cdk1-dependent inhibitory phosphorylation. *J Biol Chem.* 2009;284(8):5050–5055.
11. Kurabe N, et al. The death effector domain-containing DEDD forms a complex with Akt and Hsp90, and supports their stability. *Biochem Biophys Res Commun.* 2010;391(4):1708–1713.
12. Pende M, et al. Hypoinsulinaemia, glucose intolerance and diminished beta-cell size in S6K1-deficient mice. *Nature.* 2000;408(6815):994–997.
13. Paria BC, Huet-Hudson YM, Dey SK. Blastocyst's state of activity determines the "window" of implantation in the mouse receptive uterus. *Proc Natl Acad Sci U S A.* 1993;90(21):10159–10162.
14. Lim H, et al. Multiple female reproductive failures in cyclooxygenase 2-deficient mice. *Cell.* 1997;91(2):197–208.
15. Bany BM, Schultz GA. Tissue inhibitor of matrix metalloproteinase-3 expression in the mouse uterus during implantation and artificially induced decidualization. *Mol Reprod Dev.* 2001;59(2):159–167.
16. Hassan MQ, et al. HOXA10 controls osteoblastogenesis by directly activating bone regulatory and phenotypic genes. *Mol Cell Biol.* 2007;27(9):3337–3352.
17. Lee KY, et al. Bmp2 is critical for the murine uterine decidual response. *Mol Cell Biol.* 2007;27(15):5468–5478.
18. Diehl JA, Cheng M, Roussel MF, Sherr CJ. Glycogen synthase kinase-3beta regulates cyclin D1 proteolysis and subcellular localization. *Genes Dev.* 1998;12(22):3499–3511.
19. Das SK. Regional development of uterine decidualization: molecular signaling by Hoxa-10. *Mol Reprod Dev.* 2010;77(5):387–396.
20. Das SK, Lim H, Paria BC, Dey SK. Cyclin D3 in the mouse uterus is associated with the decidualization process during early pregnancy. *J Mol Endocrinol.* 1999;22(1):91–101.
21. García-Morales P, Hernando E, Carrasco-García E, Menéndez-Gutiérrez MP, Saceda M, Martínez-Lacaci I. Cyclin D3 is down-regulated by rapamycin in HER-2-overexpressing breast cancer cells. *Mol Cancer Ther.* 2006;5(9):2172–2181.
22. Sachs L, Shelesnyak MC. The development and suppression of polyploidy in the developing and suppressed deciduoma in the rat. *J Endocrinol.* 1955;12(2):146–151.
23. Ansell JD, Barlow PW, McLaren A. Binucleate and polyploid cells in the decidua of the mouse. *J Embryol Exp Morphol.* 1974;31(1):223–227.
24. Moulton BC. Effect of progesterone on DNA, RNA and protein synthesis of deciduoma cell fractions separated by velocity sedimentation. *Biol Reprod.* 1979;21(3):667–672.
25. Edgar BA, Orr-Weaver TL. Endoreplication cell cycles: more for less. *Cell.* 2001;105(3):297–306.
26. Yang ZZ, et al. Protein kinase B alpha/Akt1 regulates placental development and fetal growth. *J Biol Chem.* 2003;278(34):32124–32131.
27. Hirota Y, Daikoku T, Tranguch S, Xie H, Bradshaw HB, Dey SK. Uterine-specific p53 deficiency confers premature uterine senescence and promotes preterm birth in mice. *J Clin Invest.* 2010;120(3):803–815.
28. Sicinska E, et al. Requirement for cyclin D3 in lymphocyte development and T cell leukemias. *Cancer Cell.* 2003;4(6):451–461.
29. Franke TF, Kaplan DR, Cantley LC. PI3K: downstream AKTion blocks apoptosis. *Cell.* 1997;88(4):435–437.
30. Burgering BM, Coffey PJ. Protein kinase B (c-Akt) in phosphatidylinositol-3-OH kinase signal transduction. *Nature.* 1995;376(6541):599–602.
31. Franke TF. Intracellular signaling by Akt: bound to be specific. *Sci Signal.* 2008;1(24):pe29.
32. Brown C, et al. Subfertility caused by altered follicular development and oocyte growth in female mice lacking PKBalpha/Akt. *Biol Reprod.* 2010;82(2):246–256.
33. Easton RM, et al. Role for Akt3/protein kinase Bgamma in attainment of normal brain size. *Mol Cell Biol.* 2005;25(5):1869–1878.
34. Peng XD, et al. Dwarfism, impaired skin development, skeletal muscle atrophy, delayed bone development, and impeded adipogenesis in mice lacking Akt1 and Akt2. *Genes Dev.* 2003;17(11):1352–1365.
35. Simón C, Moreno C, Remohí J, Pellicer A. Cytokines and embryo implantation. *J Reprod Immunol.* 1998;39(1–2):117–131.
36. Tan Y, et al. HB-EGF directs stromal cell polyploidy and decidualization via cyclin D3 during implantation. *Dev Biol.* 2004;265(1):181–195.
37. Kodama A, et al. Progesterone decreases bone morphogenetic protein (BMP) 7 expression and BMP7 inhibits decidualization and proliferation in endometrial stromal cells. *Human Reprod.* 2010;25(3):751–756.